Research on Frequency Regulation with Dynamic Trajectory Planning of Participation Factors

Hongbin Hu[1], Jiayu Zhao[2,*], Qiang Li[3], Zhibin Jing[3], Qi Guo[3] and Zhihao Yang[3]

[1]*Inner Mongolia Power (Group) Co., Ltd., Inner Mongolia Power Research Institute Branch, Hohhot 010020, China*
[2]*Control and computer engineering school, North China Electric Power University, 102206, China*
[3]*Dispatching and Control Center of Inner Mongolia Power (Group) Co., LTD, Hohhot 010020, China*
E-mail: 19801339692@163.com
[*]*Corresponding Author*

Received 11 May 2024; Accepted 19 June 2024

Abstract

The energy transformation has led to a high proportion of new energy entering the grid. New energy has high randomness, which challenges the frequency stability of the power system. A new approach to improve frequency based on dynamic trajectory planning of participation factors is proposed in this work. In the frequency regulation interval, the trajectory and termination time of participation factors are regarded as the variables to be optimized. Then, taking the frequency regulation performance and economy as the goals, a multi-objective optimization problem is constructed. The participation factors are used to dispatch the output power of different units, which breaks the constraint that the output characteristics of different units are consistent in the original regulation process. Therefore, the generator units with different

Distributed Generation & Alternative Energy Journal, Vol. 39_4, 751–776.
doi: 10.13052/dgaej2156-3306.3943

regulation characteristics in the system achieve complementary coordination on the second time scale. In simulation cases, frequency oscillation is reduced, while the overall economy of the system is improved. The numerical evaluation results show that the frequency performance is improved by 2.7% at most and 2.9% of the economy is improved at most simultaneously. The above results demonstrate the effectiveness of the proposed approach.

Keywords: Frequency control, automatic generation control, optimal scheduling, path planning, system improvement.

1 Introduction

Frequency is one of the most essential indicators for the secure operation of power systems. The frequency should be a fixed value or have a small range of variation. In power systems, load frequency control (LFC) is usually used to achieve the balance between generated power and load consumption [1, 2]. When there are energy power generating sources like as wind, solar, coal-fired power, and others in the system, the matter of multi-machine coordinated control inevitably arises in the LFC process. In the process of China's energy transformation, the large reduction of synchronous motors leads to the decline of frequency regulation performance [3]. In addition, coal-fired power units, which make up about half of installed capacity, actively carry out flexibility transformation. Existing researches show that after the flexibility transformation, the power regulation characteristics and coal consumption characteristics of coal-fired power units will change significantly in a wide range of operating conditions [3–5]. In addition, all kinds of energy power generation are gradually increasing. These phenomena further aggravate the complexity of multi-machine coordinated control, leading to the difficulty of maintaining frequency stability. Therefore, how to enhance the coordination among various units to improve the frequency stability of a novel system is the current research focus [6, 7].

In a centralized control system, controllers and participation factors synergistically determine the outputs of different units and the performance of frequency regulation. Usually, controllers are major research objects to be optimized in previous works [8–12]. From the literature review, few researchers are focusing on the optimization of participation factors. In the traditional power market, participation factors are usually set to the same value [13]. With the reform of the power market, the economy in the regulation process is introduced gradually into the multi-machine coordination

problem by independent system operators (ISOs). A modified automatic generation control (AGC) scheme with three types of transactions is described in [14], including contracts for area regulation, poolco based transactions, and bilateral transactions. Donde et al. consider the participation of different units in frequency regulation and peak shaving regulation in different power grids [15]. Disco participation matrix (DPM) and contract participation factor (CPF) are first introduced. For this model, Debbarma [16] and Parmar [17] respectively introduce fractional order PID and optimal output feedback controller with a pragmatic viewpoint. Zhao et al presents a stochastic optimization decision-making model, which calculates the optimal AGC capacity requirement [18]. In these studies, controllers dominate the regulation performance, while participation factors only play the role of power distribution and cannot play the role of regulation optimization.

Boonchuay suggests an effective LFC strategy using levels of critical load determined by adaptive participation factors, with the locational marginal pricing (LMP) taken into consideration [19]. Participation factors can be modified on the minute-level time scale to satisfy the load limit after security constrained economic dispatch. Then the stability of this kind of adaptive LFC method is proved [20]. In economic dispatch, the cost and constraints of frequency regulation are taken into account, in which AGC and dispatch are considered as a whole optimal question [21–25]. LFC in the power market adopts distributed economic model predictive control (MPC) [23]. Accordingly, a data-driven distributionally robust optimization technique is presented that utilizes the correlations among load power, the AGC signal and variations in renewable generation [24]. Participation factors in the standard industry-employed AGC are proved to be economically optimal in load-change scenarios on the minute-level time scale, while comparison of the frequency regulation performance is ignored [25]. The essence of centralized multi-machine system coordinated control is to design an active power distribution scheme. Economic dispatch or some boundary conditions are mainly combined in previous studies, and participation factors are determined above a minute-level time scale in advance before LFC response, in which each unit can provide a fixed proportion of electricity. Then the participation factors are continuously updated in the next stage. In fact, this is a quasi-steady state algorithm similar to economic scheduling, which limits the space for further optimization of each unit. The optimal computation of participation factors has been studied to improve the flexibility and selectivity of current AGC systems [26]. The optimized participation factors are used for power flow control and a machine learning (ML) approach is employed.

The regulation effects in the regulation process are also influenced by participation factors except optimized controllers. However, to the best of our knowledge, participation factors are rarely used as a means of performance optimization. Therefore, this work introduces the method of participation factors optimization to solve the multi-machine complementary coordination problem. It is the first time that the participation factors play a role in the second-level time scale regulation process. Consequently, the main contributions of this article are the following.

1. In the process of regulating frequency, the participating factors fully utilize the complementary features of units with a variety of regulation capabilities.
2. Dynamic trajectory planning of participation factors is designed.
3. The proposed method simultaneously optimizes speed and economy of the regulation process.

The remainder of the paper is structured as follows. The problem to be solved is proposed in Section 2. The problem is described mathematically in Section 3, and a multi-objective optimization problem with dynamic trajectory planning is constructed. There is a case in Section 4. The paper is finally concluded in Section 5.

2 Problem Description

Generally, the frequency regulation process would have a similar form as Figure 1 shown. Before a load disturbance or a new-desired generation

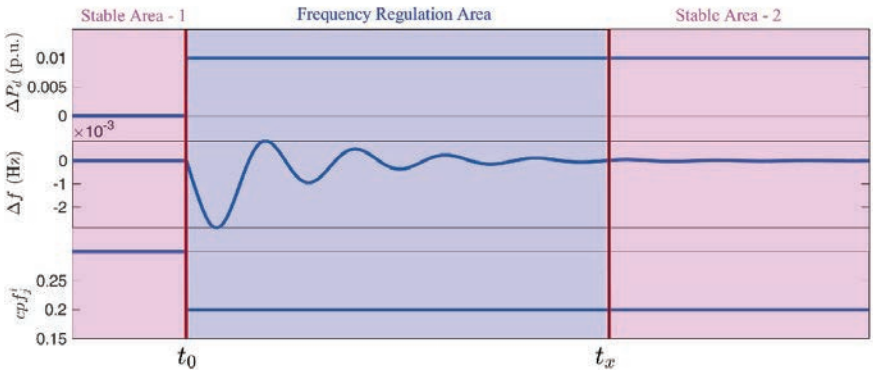

Figure 1 General process of frequency regulation.

set-point happens, the system is assumed to be stable, named Stable Area-1. Once the balance of active power is disturbed at t_0, $\Delta P_{\mathrm{d}}(s)$ is appearing. Then the frequency deviations of this area come into being. At the same time, the primary control and the second control adjust the outputs of generation units. Since each unit has different adjustment characteristics and costs, participation factors vary from each other. After regulation, the frequency would tend towards equilibrium at t_x. The regulation process between t_0 and t_x is named as Frequency Regulation Area (FRA) in this work. The regained stable state after t_x is called Stable Area-2. In Stable Area-1 and 2, each participation factor determines the proportions of each generation unit for supplying varying loads, which would influence the operation economy of the whole system for a long time. Obviously, the participation factors in stable area should be calculated and determined by security constrained economic dispatch in previous studies as follows.

$$cpf_j^i(t) = \begin{cases} \mathring{\lambda}_j^i & t \le t_0 \\ \hat{\lambda}_j^i & t \ge t_0 \end{cases} \tag{1}$$

where $\mathring{\lambda}_j^i$ and $\hat{\lambda}_j^i$ are fixed values of unit j in control area i, which is determined by economic dispatch, and $\forall j \in (1, \ldots n)$, is the number of units in area i.

However, in previous works and engineering as stated above, the values of participation factors in FRA are assumed to be constants. Can it be used to improve the adjustment effect? In this work, improvements in frequency regulation with the help of the optimization of participation factors in FRA would be first discussed and a solution would be proposed.

3 Proposed Approach

3.1 Modeling and Proposed Approach

The linear models of LFC can be found in quite a lot literature. A multi-area centralized control system's state-space representation can be expressed as

$$\begin{cases} \dot{x}_i(t) = A_i x_i(t) + B_i u_i(t) + B_{wi} w_i(t) \\ y_i(t) = C_i x_i(t) \end{cases} \tag{2}$$

Where

$$x_i(t) = [f^i \Delta P^{i,k}_{tie} \Delta P^i_{v,1} \dots P^i_{v,n} \Delta P^i_{t,1} \dots \Delta P^i_{t,n}[]^T]$$

$$A_i = \begin{bmatrix} -\frac{D^i}{2H^i} & 0 & 0 & \dots & 0 & \frac{1}{2H^i} & \dots & \frac{1}{2H^i} \\ 2\pi \sum_{k=1,k\neq i}^{n} C_{ik} & 0 & 0 & \dots & 0 & 0 & \dots & 0 \\ -\frac{1}{T^i_{g,1}R^i_1} & 0 & -\frac{1}{T^i_{g,2}} & \dots & 0 & 0 & \dots & 0 \\ & & & \vdots & & & & \\ -\frac{1}{T^i_{g,n}R^i_n} & 0 & 0 & \dots & -\frac{1}{T^i_{g,n}} & 0 & \dots & 0 \\ 0 & 0 & \frac{1}{T^i_{T,1}} & \dots & 0 & -\frac{1}{T^i_{T,1}} & \dots & 0 \\ & & & \vdots & & & & \\ 0 & 0 & 0 & \dots & \frac{1}{T^i_{T,n}} & 0 & \dots & -\frac{1}{T^i_{T,n}} \end{bmatrix}$$

$$B_i = \begin{bmatrix} 0 & 0 & \frac{cpf^i_1}{T^i_{g,1}} & \dots & \frac{cpf^i_n}{T^i_{g,n}} & 0 & \dots & 0 \end{bmatrix}^T$$

$$B_{wi} = \begin{bmatrix} \frac{1}{2H^i} & 0 & 0 & \dots & 0 \\ 0 & -2\pi & 0 & \dots & 0 \end{bmatrix}^T$$

$$C_i = \begin{bmatrix} B^i & 1 & 0 & \dots & 0 \end{bmatrix}^T$$

$$w_i = \begin{bmatrix} \Delta P^i_d & \sum_{k=1,k\neq i}^{n} C_{ik} \Delta f^k \end{bmatrix}^T$$

where the symbols with superscript i represents the objects in control area i, the symbols with subscript j represents the different number of unit in

the area, Δf^i is frequency deviation, $\Delta P_{tie}^{i,k}$ is the tie-line power exchange between the area i and k, $\Delta P_{v,j}^i$ is the turbine value position deviation, $\Delta P_{t,j}^i$ is the generator mechanical power deviation, D_i is the damping coefficient of the generator, H_i is moments of inertia of the generator, C_{ik} is the tie-line synchronizing coefficient between the area i and k, $T_{g,j}^i$ is time constant of the governor, $T_{T,j}^i$ is time constant of the turbine, R_j^i is the speed droop, B^i is frequency bias factor, and ΔP_d^i is load deviation. In addition, ACE^i is the input of the controller, $ACE^i = B^i \Delta f^i + \Delta P_{tie}^{i,k}$. The traditional controller $u = K_p^i \bullet ACE^i + K_I^i \int ACE^i dt$is employed in this work, where K_P^i and K_I^i are the controller's parameters in control area i.

In a process of frequency regulation process, the most important objective is to maintain the frequency within a narrow range or at a specific fixed value by LFC as quickly as possible. As the statement in the previous section, the first objective of optimization in FRA must be listed as

$$f_1 = Min\left(\int (|\Delta f^i| + |\Delta P_{tie}^{i,k}|)dt\right) \tag{3}$$

After the performance of frequency response is guaranteed, the economy of operation could also be considered in the regulation process. Naturally, the second objective of optimization in FRA can be listed as:

$$f_2 = Min\left(\gamma_1 \int \Delta P_{t,1}^i dt + \gamma_2 \int \Delta P_{t,2}^i dt + \cdots \gamma_n \int \Delta P_{t,n}^i dt\right) \tag{4}$$

where γ_j represents the cost or electricity price of unit j in the market.

As stated above, the numerical values of participation factors in FRA would change the frequency response performance. Therefore, these values in FRA are ones of the variables which need to be optimized. In the regulation process, numerical values change along with time. At the end of FRA, the variations of participation factors should gradually decrease. It's a natural association that figuring out when FRA ends is equally essential. Here, the duration of frequency oscillation is assumed to be represented as $(t_x - t_0)$. Equation (2) could then be modified as follows:

$$cpf_j^i(t) = \begin{cases} \mathring{\lambda}_j^i & t \le t_0 \\ \mu_j^i(t) & t_0 < t < t_x \\ \hat{\lambda}_j^i & t \ge t_x \end{cases} \tag{5}$$

where $\mu_j^i(t)$ represents the numerical values of participation factors of unit j in control area i at time t in FRA, which varies with time t.

In the optimized process, the following constraints should also be satisfied:

(1) The constraints of participation factors at the end of Frequency Regulation Area: When the time is approaching to t_x, to prevent the oscillation of frequency caused by jumping of factors at t_x, $\mu_j^i(t)$ should be equal to the values set by economic dispatch approximately.

$$\mu_j^i(t_x) = \hat{\lambda}_j^i \tag{6}$$

More stringently, the following constraints could be considered to guarantee a smoother switch at t_x further.

$$\lim_{t \to t_x} \frac{\partial \mu_j^i(t)}{\partial t} = 0 \tag{7}$$

(2) Generation units' outputs limit constraints: Each unit's generation output should be constrained by a realistic output limitation.

$$P_{T,j}^{i,min} \leq P_{t,j}^i \leq P_{t,j}^{i,max} \tag{8}$$

(3) The limit on variable load rate: There are limits on speed limit during load change of units.

$$\frac{\partial \triangle P_{t,j}^i}{\partial t} < \xi_j \tag{9}$$

where ξ_j is the upper limit of the climbing rate of unit j.

(4) Regulation time constraints: The length of time of FRA must be a positive value, and theoretically there is no upper limit.

$$t_x - t_0 > 0 \tag{10}$$

In FRA, the longest adjustment time t_p can be manually set to allow as follows.

$$t_p > t_x - t_0 \tag{11}$$

(5) Summation constraint of participation factors: Usually, in the process of designing and solving participation factors in the past, the total of the participation factors should be equal to 1 in the same area as follows.

$$\sum_j cpf_j^i = 1 \tag{12}$$

Due the re-planning problem of participation factors would be solved in this work, this constraint can be relaxed in FRA for a short time theoretically. Then in the Stable Area-2, the constraints that the sum of participation factors is 1 can be achieved again. Hence, the summation constraint of participation factors in FRA is cancelled, which would unavoidably result in a rise in the number of variables for decision-making in each area.

In conclusion, the problem of using participation factors redesign to improve the effect of frequency regulation can be abstracted as a multi-objective trajectory planning optimization problem. Especially, the end time of trajectory planning is also a decision variable.

3.2 Trajectory Planning of Participation Factors

In the previous section, an approach to improve frequency regulation by utilizing participation factors is introduced and abstracted. Except the above part, an essential part of this approach has not been solved. That's how to design the dynamic trajectory planning of participation factors in FRA. Exactly, there are several methods to complete the task. Therefore, this section is designed to be independent from the previous section to guarantee the universality of the proposed approach. In this work, a common method is employed to resolve the problem.

First, the question is described with Figure 2 in this section more specifically. In control area i, the points of participation factors, cpf_j^{i} have

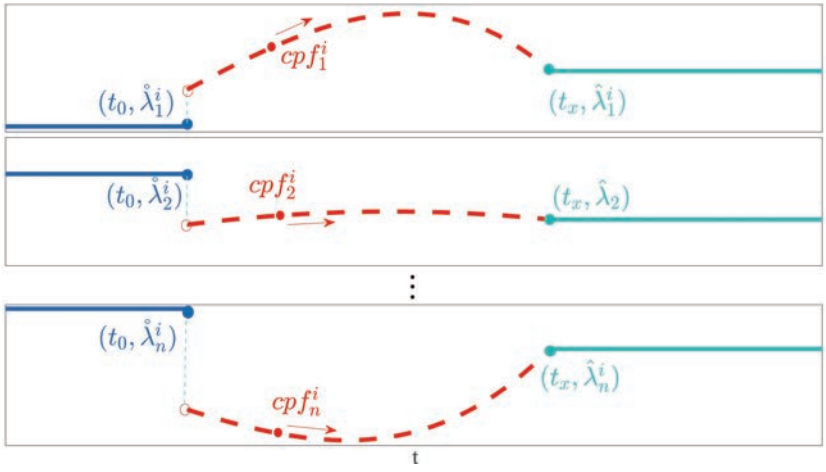

Figure 2 The diagram of trajectory planning.

to be designed from starting points at t_0 to move to terminal points at (t_x, $\hat{\lambda}_j^i$). The trajectories are optimized variables and represented as $\mu_j^i(t)$ in Equation (5). Also, the time of terminal points, t_x, is another variable to be optimized. Optimization objectives are listed as Equations (3) and (4).

Usually, a continuous trajectory could be described by a polynomial [27, 28] as following:

$$\mu_j^i(t) = q_{j,0}^i + q_{j,1}^i t + q_{j,2}^i t^2 + \cdots q_{j,m}^i t^m, t_0 < t < t_x \tag{13}$$

where $q_{j,l}^i$ are unknown parameters, $l \in [0, m]$.

If a vector is introduced as following:

$$\boldsymbol{q}_j^i = [q_{j,0}^i, q_{j,1}^i \ldots q_{j,m}^i]^T \tag{14}$$

Then Equation (13) can be further derived as

$$\mu_j^i(t) = [1, t, t^2 \ldots t^m]\boldsymbol{q}_j^i, t_0 < t < t_x \tag{15}$$

However, in practical application, a polynomial is too simple to describe an irregular trajectory. So, without loss of generality, each trajectory of participation factors is described by multiple polynomials as following:

$$\mu_j^i(t) = \begin{cases} [1, t, t^2, \ldots, t^m]\boldsymbol{q}_{j,1}^i, \ t_0 < t < t_1 \\ [1, t, t^2, \ldots, t^m]\boldsymbol{q}_{j,2}^i, \ t_1 < t < t_2 \\ \ldots \\ [1, t, t^2, \ldots, t^m]\boldsymbol{q}_{j,\beta}^i, \ t_{\beta-1} < t < t_0 + t_x \end{cases} \tag{16}$$

where β represents the number of segments, $\beta \geq 1$.

Therefore, the optimization problem in this work can be described as following finally.

$$\underset{\boldsymbol{q}_{j,\beta}^i \in \mathbf{R}, t_x - t_0 \in R^+}{Min} \left(\int (|\Delta f^i| + |\Delta P_{tie}^{i,k}|) dt \right) \tag{17}$$

$$\underset{\boldsymbol{q}_{j,\beta}^i \in \mathbf{R}, t_x - t_0 \in R^+}{Min} \left(\gamma_1 \int \Delta P_{t,1}^i dt + \cdots + \gamma_n \int \Delta P_{t,n}^i dt \right) \tag{18}$$

$$s.t. \ \mu_j^i(t_x) = \hat{\lambda}_j^i \tag{19}$$

$$\Sigma \mu_j^i(t_x) = 1 \tag{20}$$

$$P_{t,j}^{i,min} \leq P_{t,j}^{i} \leq P_{t,j}^{i,max} \tag{21}$$

$$\frac{\partial \triangle P_{t,j}^{i}}{\partial t} < \xi \tag{22}$$

$$\mu_j^i(t) = \begin{cases} [1, t, t^2, \ldots, t^m]\boldsymbol{q}_{j,1}^i, \ t_0 < t < t_1 \\ [1, t, t^2, \ldots, t^m]\boldsymbol{q}_{j,2}^i, \ t_1 < t < t_2 \\ \ldots \\ [1, t, t^2, \ldots, t^m]\boldsymbol{q}_{j,\beta}^i, \ t_{\beta-1} < t < t_0 + t_x \end{cases} \tag{23}$$

$$i = 1 \ldots h \tag{24}$$

$$j = 1 \ldots n \tag{25}$$

$$l = 1 \ldots m \tag{26}$$

To solve the above multi-objective optimization issue, this work employs a non-dominated sorting genetic algorithm II (NSGA2)[29]. q_j^i and t_x are set as variables to be optimized for NAGA2. First, a randomly generated initial population of size N is created. The three fundamental genetic algorithmic processes of selection, crossover, and mutation are used to produce the first-generation offspring population after non-dominant sorting. Secondly, starting with the second generation, the parent and offspring populations are combined for quick non-dominated sorting. Concurrently, the degree of crowding for every individual in every non-dominated layer is computed, and appropriate individuals are chosen to construct a new parent population based on the individual crowding degree and the non-dominated relationship. Next, create new offspring populations by applying the fundamental principles of genetic algorithms until the required number of iterations needed is attained. In the end, q_j^i and t_x can be determined and the optimization issue can be resolved.

3.3 System Design

On the basis of above derivation, a whole modified procedure in LFC is designed to be updated in Figure 3. Day-ahead dispatch and ISOs give the planned power ($P_{dispatch}$) and contract participation factor (cpf) via energy management system (EMS). When there is no disturbance, the power setting value ($P_{setpoint}$) is equal to the dispatching instruction and remains unchanged. If an obvious load mismatch (ΔP) is detected, then turn to the optimization; the margin, ε, can be specified as a low value. The modified

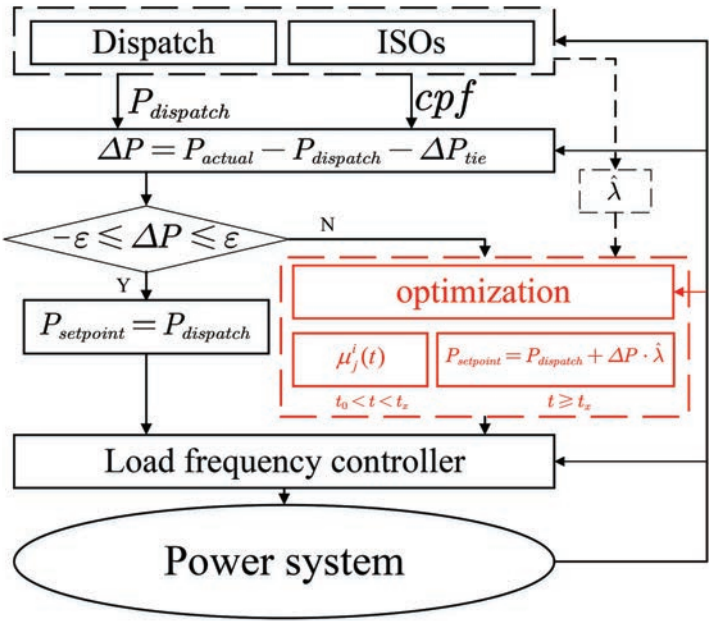

Figure 3 Modified procedure of optimization in LFC.

part compared with the conventional approach is represented by the region with a red color in Figure 3. After optimization, Equation (5) is sent to the load frequency controller, including $\mu_j^i(t)$, t_x, and new power setting value from ISOs. Thus, the dynamic regulation process would be improved and the operation economy would also be guaranteed.

However, the solution of the optimization algorithm requires a lot of time, especially involving the solution of large-scale power grid. This drawback of the algorithm is difficult to meet real-time applications. Therefore, the engineering application of this method requires high calculation speed and may be realized in the future. In addition, at the current stage, case-based reasoning (CBR) can be used to gradually realize the engineering application of this method. The specific assumptions are as follows: 1. Find the typical power grid operation mode and frequency deviation generation mode in the historical database; 2. For these typical working conditions, the corresponding results are obtained by off-line optimization, and a data table can be established; 3. Develop a distance judgment algorithm to judge different working conditions; 4. If it is the typical working conditions, related data in the data table can be used to realize real-time automatic operation.

4 Case Study

As shown in Figure 4, to demonstrate how well the suggested algorithm is, the model in reference [30] is chosen as a test platform. Table 1 contains the three-area model's parameters. The optimal parameters of PI controllers can be referred to as [−0.000327, −0.3334; −0.000696, −0.3435; −0.00016, −0.3398]. The original participation factors can be found as follows:

$$\begin{bmatrix} \mathring{\lambda}_1^1 & \mathring{\lambda}_2^1 & \mathring{\lambda}_3^1 \\ \mathring{\lambda}_1^2 & \mathring{\lambda}_2^2 & \mathring{\lambda}_3^2 \\ \mathring{\lambda}_1^3 & \mathring{\lambda}_2^3 & \mathring{\lambda}_3^3 \end{bmatrix} = \begin{bmatrix} 0.4 & 0.4 & 0.2 \\ 0.6 & 0 & 0.4 \\ 0 & 0.5 & 0.5 \end{bmatrix}$$

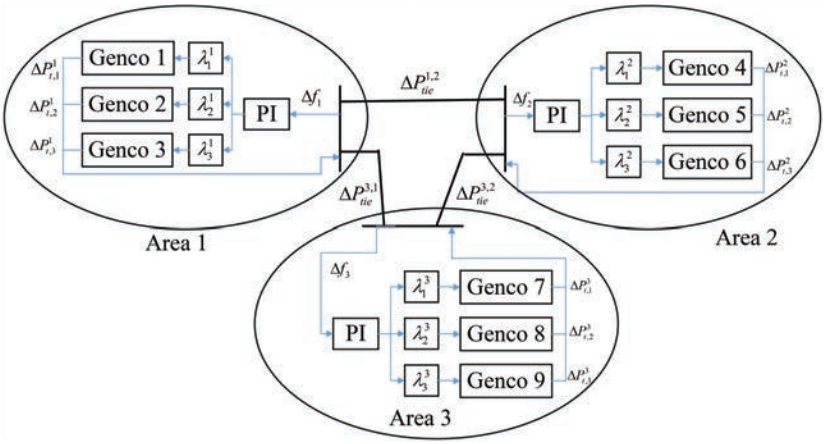

Figure 4 Three-area model.

Table 1 Parameters of three-area model

Parameters	Units								
MVAbase (1000 MW)	1	2	3	4	5	6	7	8	9
Rate(MW)	1000	800	1000	1100	900	1200	850	1000	1020
D(p.u./Hz)	0.015	0.014	0.015	0.016	0.014	0.014	0.015	0.016	0.015
H(pu.sec)	0.08335	0.06	0.1	0.010085	0.075	0.098	0.06235	0.08335	0.0935
TT(sec)	0.4	0.36	0.42	0.44	0.32	0.4	0.3	0.4	0.41
Tg(sec)	0.08	0.06	0.07	0.06	0.06	0.08	0.07	0.07	0.08
R(Hz/pu)	3	3	3.3	2.7273	2.6667	2.5	2.8235	3	2.9412
B(pu/Hz)	0.3483	0.3473	0.3180	0.3827	0.3890	0.414	0.3692	0.3493	0.355
cpf	0.4	0.4	0.2	0.6	0	0.4	0	0.5	0.5
ξ	8	8	4	12	0	8	0	10	10

Now, the load disturbances are assumed as $\Delta P_d^1 = -0.1\ pu$, $\Delta P_d^2 = -0.1\ pu$, $\Delta P_d^3 = 0.05\ pu$ at 10 s. New participation factors after 10 s are set by ISOs, which are assumed as follows:

$$\begin{bmatrix} \hat{\lambda}_1^1 & \hat{\lambda}_2^1 & \hat{\lambda}_3^1 \\ \hat{\lambda}_1^2 & \hat{\lambda}_2^2 & \hat{\lambda}_3^2 \\ \hat{\lambda}_1^3 & \hat{\lambda}_2^3 & \hat{\lambda}_3^3 \end{bmatrix} = \begin{bmatrix} 0.3 & 0.4 & 0.3 \\ 0.2 & 0.4 & 0.4 \\ 0.2 & 0.6 & 0.2 \end{bmatrix}$$

In addition, the market cost of each unit is needed in these situations. The economy results of the whole system would be influenced by the relative cost of different units. The costs are assumed as follows:

$$\begin{bmatrix} \gamma_1^1 & \gamma_2^1 & \gamma_3^1 \\ \gamma_1^2 & \gamma_2^2 & \gamma_3^2 \\ \gamma_1^3 & \gamma_2^3 & \gamma_3^3 \end{bmatrix} = \begin{bmatrix} 0.13 & 0.1 & 0.1 \\ 0.1 & 0.05 & 0.09 \\ 0.05 & 0.12 & 0.1 \end{bmatrix}$$

The operation costs of unit 5 and unit 7 are assumed to be the lowest. However, units 2, 5, and 7 are considered to have faster adjustment speed from the smaller time constant of their models.

4.1 Result Analysis

First, the simple trajectory is employed to verify the algorithm in this work. The following trajectory is assumed.

$$\mu_j^i(t) = [1, t]\boldsymbol{q}_j^i, t_0 < t < t_x \tag{27}$$

During optimization, the population is set to 500 and the number of iterations is set to 800. Figure 5 shows the solution space, in which point C is obtained from the process object that is not optimized by this method [30]. Figure 5 illustrates that there exist numerous options that can meet the dual improvement of system regulation stability and economy. Point A with the best frequency regulation is selected as a comparison, as well as point B with the best economics under guaranteed regulation performance. Parameters and index calculation results of three points can be seen in Table 2.

Figures 6–7 display the frequency deviation and tie-line power of point A. Participation factors and power outputs of each unit are shown in Figures 8–10, respectively. As mentioned above, unit 2 and unit 5 have faster regulation capacity, while unit 5 and unit 7 have better operation economy. Therefore, unit 5 bears the main regulation power during the regulation

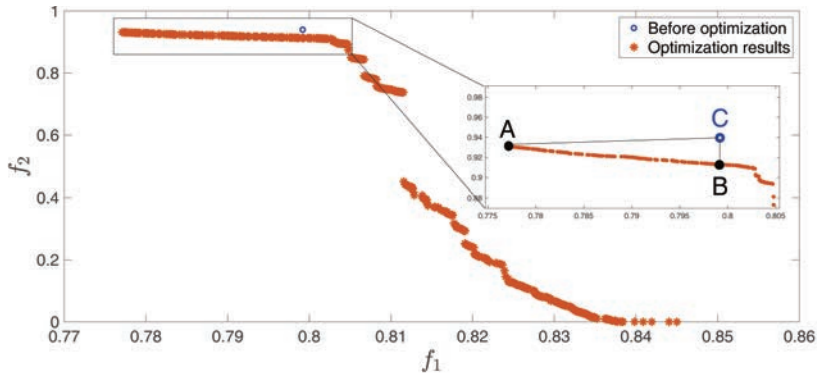

Figure 5 Pareto optimal front.

Table 2 Model parameters of three-area power system

	A	B	C
$q^1_{1,0}$	−6.9829	−7.2544	\
$q^1_{2,0}$	5.6427	6.7316	\
$q^1_{3,0}$	2.2417	2.3697	\
$q^2_{1,0}$	−1.4540	−1.4127	\
$q^2_{2,0}$	6.5162	9.2188	\
$q^2_{3,0}$	−3.1043	−5.2486	\
$q^3_{1,0}$	9.9762	10	\
$q^3_{2,0}$	−5.4631	−5.6331	\
$q^3_{3,0}$	5.5401	8.8831	\
t_x	11.7359	12.9925	\
f_1	0.7771	0.7992	0.7992
f_2	0.9313	0.9120	0.9395

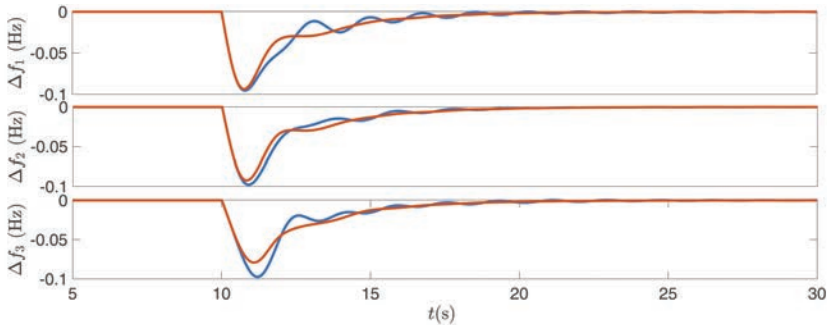

Figure 6 Comparison results of frequency deviation between point A and point C. Point A is represented by the red line, and point C by the blue line.

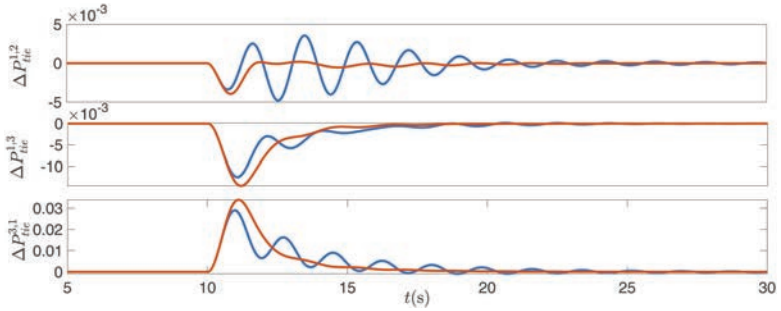

Figure 7 Comparison results of tie-line power between point A and point C. Point A is represented by the red line, and point C by the blue line.

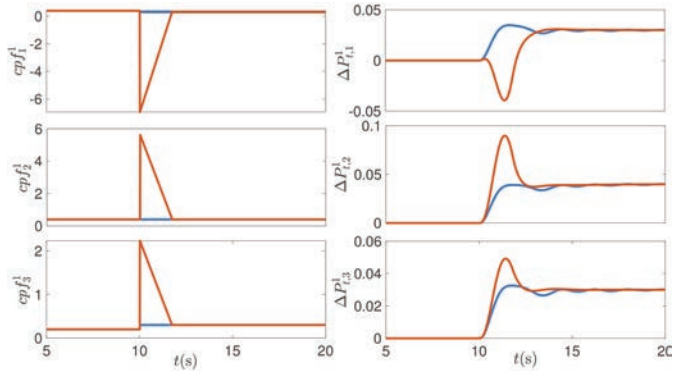

Figure 8 Comparison results of participation factors and power outputs of unit 1-3 between point A and point C. Point A is represented by the red line, and point C by the blue line.

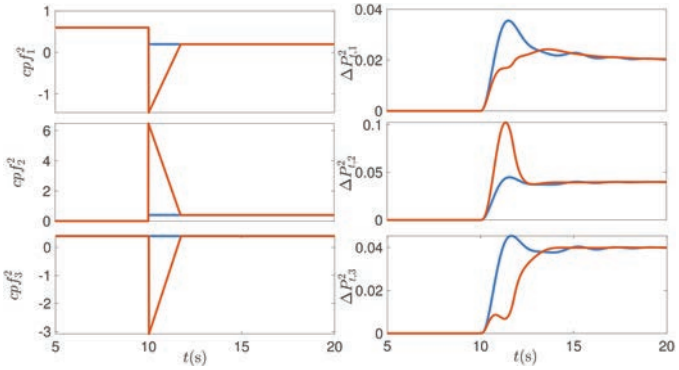

Figure 9 Comparison results of participation factors and power outputs of unit 4-6 between point A and point C. Point A is represented by the red line, and point C by the blue line.

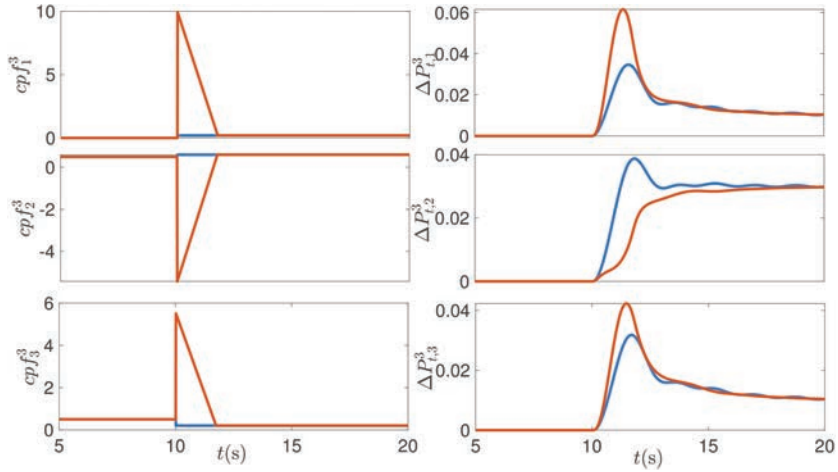

Figure 10 Comparison results of participation factors and power outputs of unit 7-9 between point A and point C. Point A is represented by the red line, and point C by the blue line.

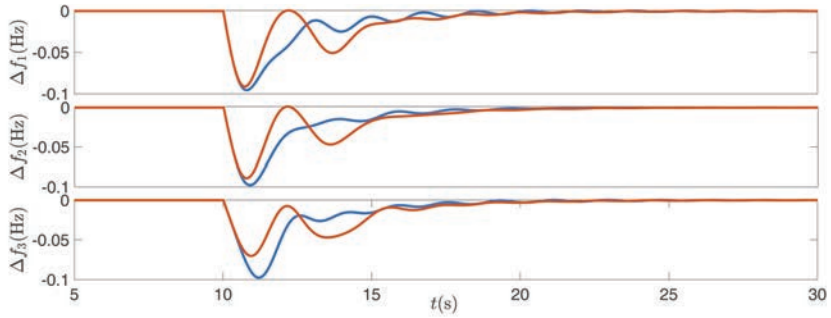

Figure 11 Comparison results of frequency deviation between point B and point C. Point B is represented by the red line, and point C by the blue line.

process, which can be verified in the figures. At the same time, unit 1 has poor economy and general regulation rate, so it can be seen that the output of unit 1 first decreases and then rises to the output specified by the ISOs. During the complementary regulation of each unit in point A, the frequency regulation performance is improved from 0.7992 to 0.7771, while the economy of the whole process has been slightly improved.

Figures 11–12 display the frequency deviation and tie-line power of point B. Participation factors and power outputs of each unit are shown in Figures 13–15, respectively. The adjustment time of point B is a little longer

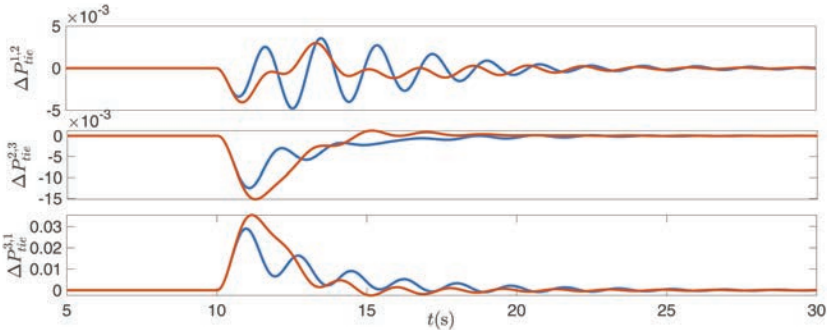

Figure 12 Comparison results of tie-line power between point B and point C. Point B is represented by the red line, and point C by the blue line.

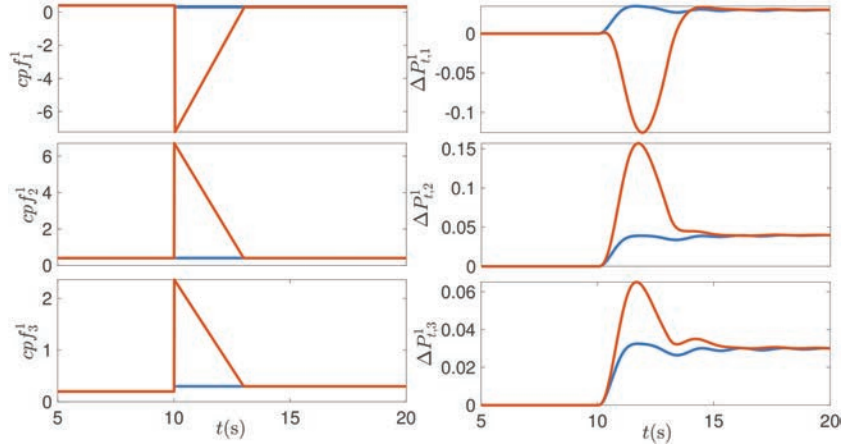

Figure 13 Comparison results of participation factors and power outputs of units 1-3 between point B and point C. Point B is represented by the red line, and point C by the blue line.

than that of point A. The overall operation trend of all units in point B is similar to point A. In point B, the frequency regulation performance of the system does not degrade, while the economy of the whole process is improved from 0.9395 to 0.9120.

4.2 Stability Analysis

In order to confirm the stability of the algorithm, the Monte Carlo simulation technique is applied to randomize the parameters of the power distribution

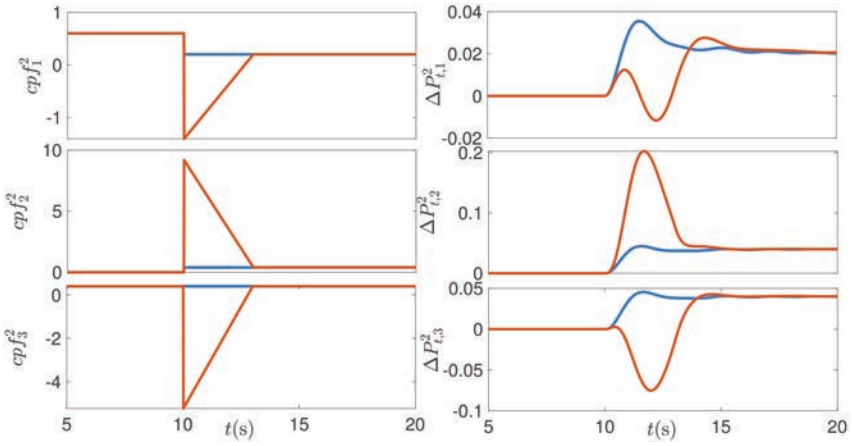

Figure 14 Comparison results of participation factors and power outputs of units 4-6 between point B and point C. Point B is represented by the red line, and point C by the blue line.

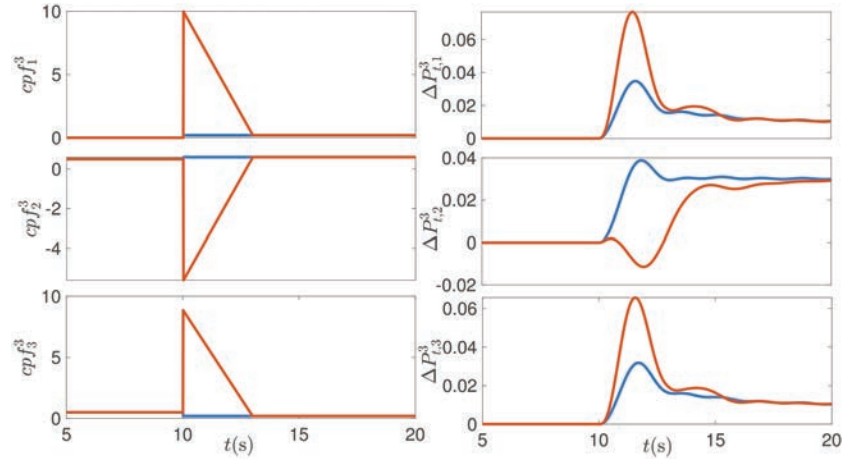

Figure 15 Comparison results of participation factors and power outputs of units 7-9 between point B and point C. Point B is represented by the red line, and point C by the blue line.

factor in the oscillation area. The specific parameters are set as follows.

$$t_p = 50s \tag{28}$$

$$\mu_j^i(t) = 10 \times (rand - 0.5), t \in [10, t_p] \tag{29}$$

$$t_x = (800 \times (rand - 0.5)/10 + 10) \tag{30}$$

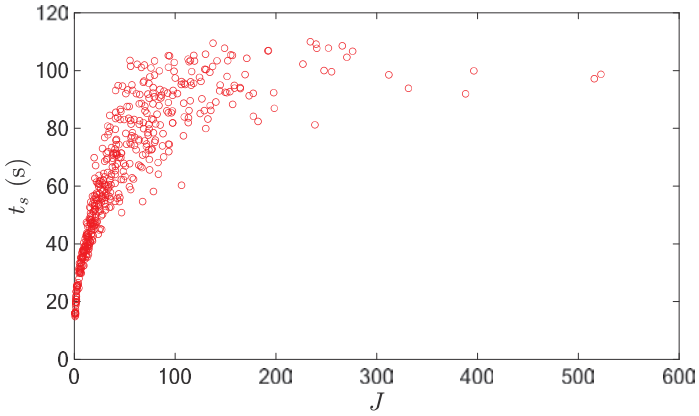

Figure 16 Result of Monte Carlo simulations.

At 10 s, the load disturbances in Areas 1, 2, and 3 increase by 0.1, 0.1, and 0.05 pu, respectively. The total length of simulation time is 180s and the number of simulations is 500. Simulation results can be seen in Figure 16. Abscissa is the measurement index of frequency fluctuation, which is represented as Equation (31). The ordinate is the adjustment time (t_s), which means the last time when the absolute value of frequency difference reaches 0.01 Hz.

$$J_1 = \int (|\Delta f^i| + |\Delta P_{tie}^{i,k}|)dt \tag{31}$$

Monte Carlo simulation results show that no matter how the participation factors change in FRA, the system remains stable within 110 s. Actually, at the end of FRA, the system automatically transforms into a constant system controlled by PI controllers. Then the strong stability ability of PI controllers can make the system return to stability after oscillation. And in the optimization process, there must be a solution ($m = 0, q_{j,0}^i = \hat{\lambda}_j^i$) that is not weaker than the original system, which can ensure that the maximum frequency deviation or ROCOF are within the safety threshold.

5 Conclusion

In the energy transformation process of China, a high proportion of new energy is connected to the grid, while a large number of synchronous motors are withdrawn. Then the problem of frequency regulation has gradually emerged in the power system. In response to this situation, this article

proposes a new method to improve frequency based on dynamic trajectory planning of participation factors. The main conclusions formed in this article are as follows:

1. A frequency regulation model based on multi-objective optimization is constructed. In general, the system's changes in frequency in confront of load disturbance can be divided into Stable Area and FRA. The participation factors of each unit in FRA are regarded as an optimization variable for the first time in this work. Referring to the method of UAV dynamic trajectory planning, the action trajectory of participation factors in FRA is modeled. The minimum frequency fluctuation and optimal economy of the system in FRA are considered to be the optimization objectives. Thus, a multi-objective optimization problem is formulated.
2. The solution method for multi-objective optimization problem has been introduced. NAGA2 algorithm is applied to resolve the multi-objective optimization process. And the stability of the algorithm is confirmed by the Monte Carlo simulation technique.
3. Simulation is carried out to verified the method. A centralized control system of three regions and nine units is employed as the test platform. Compared with the traditional method, frequency oscillation is reduced and the overall economy of the system is improved simultaneously based on the optimized method. In case study, frequency performance is improved by 2.7% at most, while 2.9% of the economy is also improved at most without a decrease in frequency performance.

However, the solution of optimization algorithms requires a lot of time, and the real-time application of the above methods has to consider more feasible engineering implementation methods. In the future, theoretical analysis of stability will be further studied. And a more practical power grid model will be considered to get more convincing results.

Acknowledgment

The authors would like to thank Major science and technology projects in Inner Mongolia Autonomous Region of China (2021ZD0026).

References

[1] P. Kundur, "Power System Stability and Control," New York, NY, USA: McGraw-Hill, 1993.

[2] N. Rogkas, E. Karampasakis, M. Fotopoulou, et al. “Assessment of heat transfer mechanisms of a novel high-frequency inductive power transfer system and coupled simulation using FEA,” Energy, vol. 300, 131530, 2024.
[3] M. Du, Y. Niu, B. Hu, et al., “Frequency regulation analysis of modern power systems using start-stop peak shaving and deep peak shaving under different wind power penetrations,” International Journal of Electrical Power & Energy Systems, vol. 125, pp. 106501, 2021.
[4] N. Pathak, T. S. Bhatti, A. Verma and I. Nasiruddin, “AGC of Two Area Power System Based on Different Power Output Control Strategies of Thermal Power Generation,” IEEE Transactions on Power Systems, vol. 33, no. 2, pp. 2040–2052, March 2018.
[5] Z. Liu, C. Wang, J. Fan, et al., “Enhancing the flexibility and stability of coal-fired power plants by optimizing control schemes of throttling high-pressure extraction steam,” Energy, vol. 288, 129756, 2024.
[6] H. Bevrani, H. Golpîra, A. Messina, et al., “Power system frequency control: An updated review of current solutions and new challenges,” Electric Power Systems Research, vol. 194, pp. 107114, 2021.
[7] G. Sharma, N. Krishnan, Y. Arya. Impact of ultracapacitor and redox flow battery with JAYA optimization for frequency stabilization in linked photovoltaic-thermal system. International transactions on electrical energy system, 2021, 31(5):e12883.
[8] X. Liu, Y. Zhang and K. Y. Lee, “Coordinated Distributed MPC for Load Frequency Control of Power System With Wind Farms,” IEEE Transactions on Industrial Electronics, vol. 64, no. 6, pp. 5140–5150, June 2017.
[9] M. Ma, C. Zhang, X. Liu and H. Chen, “Distributed Model Predictive Load Frequency Control of the Multi-Area Power System After Deregulation,” IEEE Transactions on Industrial Electronics, vol. 64, no. 6, pp. 5129–5139, June 2017.
[10] N. Pathak and Z. Hu, “Hybrid-Peak-Area-Based Performance Index Criteria for AGC of Multi-Area Power Systems,” IEEE Transactions on Industrial Informatics, vol. 15, no. 11, pp. 5792–5802, Nov. 2019.
[11] W. Liu, J. Shen, S.C. Zhang, et al. Distributed Secondary Control Strategy Based on Q-learning and Pinning Control for Droop-controlled Microgrids. Journal of Modern Power Systems and Clean Energy, vol. 10, no. 5, pp. 1314–1325, September 2022.

[12] SR Nayak, PK Khadanga, Y. Arya. Influence of ultra-capacitor on AGC of five-area hybrid power system with multi-type generations utilizing sine cosine adopted dingo optimization algorithm. Electric power system research, 2023, 223: 109513.

[13] M. Ranjan, R. Shankar, "A literature survey on load frequency control considering renewable energy integration in power system: Recent trends and future prospects," Journal of Energy Storage, vol. 45, pp. 103717, 2022.

[14] J. Kumar, Kah-Hoe Ng and G. Sheble, "AGC simulator for price-based operation. I. A model," IEEE Transactions on Power Systems, vol. 12, no. 2, pp. 527–532, May 1997.

[15] V. Donde, M. A. Pai and I. A. Hiskens, "Simulation and optimization in an AGC system after deregulation," IEEE Transactions on Power Systems, vol. 16, no. 3, pp. 481–489, Aug. 2001.

[16] S. Debbarma, L. C. Saikia and N. Sinha, "AGC of a multi-area thermal system under deregulated environment using a non-integer controller," Electric Power Systems Research, vol. 95, pp. 175–183, 2013.

[17] K. Parmar, S. Majhi and D. Kothari, "LFC of an interconnected power system with multi-source power generation in deregulated power environment," International Journal of Electrical Power & Energy Systems, vol. 57, pp. 277–286, 2014.

[18] X. Zhao, F. Wen, D. Gan, et al., "Determination of AGC capacity requirement and dispatch considering performance penalties," Electric Power Systems Research, vol. 70, no. 2, pp. 93–98, 2004.

[19] C. Boonchuay, "Improving Regulation Service Based on Adaptive Load Frequency Control in LMP Energy Market," IEEE Transactions on Power Systems, vol. 29, no. 2, pp. 988–989, March 2014.

[20] T. Tao, S. Roy, S. Yuan, et al., "Robust Adaptation in Dynamically Switching Load Frequency Control," IFAC-PapersOnLine, vol. 53, no. 2, pp. 13460–13465, 2020.

[21] N. Li, C. Zhao and L. Chen," Connecting Automatic Generation Control and Economic Dispatch From an Optimization View," IEEE Transactions on Control of Network Systems, vol. 3, no. 3, pp. 254–264, Sept. 2016.

[22] Q. Zhou, M. Shahidehpour, Z. Li and X. Xu, "Two-Layer Control Scheme for Maintaining the Frequency and the Optimal Economic Operation of Hybrid AC/DC Microgrids," IEEE Transactions on Power Systems, vol. 34, no. 1, pp. 64–75, Jan. 2019.

[23] C. Zhang, S. Wang and Q. Zhao, "Distributed economic MPC for LFC of multi-area power system with wind power plants in the power market environment," International Journal of Electrical Power & Energy Systems, vol. 126, pp. 106548, 2021.

[24] L. Liu, Z. Hu, X. Duan and N. Pathak, "Data-Driven Distributionally Robust Optimization for Real-Time Economic Dispatch Considering Secondary Frequency Regulation Cost," IEEE Transactions on Power Systems, vol. 36, no. 5, pp. 4172–4184, Sept. 2021.

[25] S. Baros, Y. C. Chen and S. V. Dhople, "Examining the Economic Optimality of Automatic Generation Control," IEEE Transactions on Power Systems, vol. 36, no. 5, pp. 4611–4620, Sept. 2021.

[26] E. Tsydenov, A. Prokhorov, L. Wang. Online Estimation of Plant Participation Factors for Automatic Generation Control in Power Systems With Variable Energy Resources. IEEE Transactions on Industry Applications, 2022, 58(4): 4401–4410.

[27] A. Brown and D. Anderson, "Trajectory Optimization for High-Altitude Long-Endurance UAV Maritime Radar Surveillance," IEEE Transactions on Aerospace and Electronic Systems, vol. 56, no. 3, pp. 2406–2421, June,2020.

[28] P. Savsani, R. L. Jhala and V. J. Savsani, "Comparative Study of Different Metaheuristics for the Trajectory Planning of a Robotic Arm," IEEE Systems Journal, vol. 10, no. 2, pp. 697–708, June 2016.

[29] S. Schulz, J. S. Neufeld, U. Buscher, "A multi-objective iterated local search algorithm for comprehensive energy-aware hybrid flow shop scheduling," Journal of Cleaner Production, vol. 224, pp. 421–434, 2019.

[30] D. Rerkpreedapong, A. Hasanovic and A. Feliachi, "Robust load frequency control using genetic algorithms and linear matrix inequalities," IEEE Transactions on Power Systems, vol. 18, no. 2, pp. 855–861, May 2003.

Biographies

Hongbin Hu holds a master's degree and is a senior engineer at Inner Mongolia Power Research Institute Branch. And he is mainly engaged in research work on new energy technology.

Jiayu Zhao was born in Shanxi, China, in 2000. From 2018 to 2022, she studied in North China Electric Power University and received her bachelor's degree in 2022. Currently, she is studying for a master's degree in North China Electric Power University. She is mainly engaged in research on reinforcement learning and coordinated control of multi units.

Qiang Li is a senior engineer of Dispatching and Control Center of Inner Mongolia Power (Group) Co., LTD, who is mainly engaged in research work related to power system safety analysis and power system simulation.

Zhibin Jing is a senior engineer of Dispatching and Control Center of Inner Mongolia Power (Group) Co., LTD. He is mainly engaged in production and research work in the optimization and scheduling of power systems.

Qi Guo is a professor of engineering. He has rich experience in power system scheduling. And he is engaged in long-term research on operational optimization of high proportion new energy power systems.

Zhihao Yang is an expert in the operation and production of the power system, with rich experience in operation and research, and has been engaged in multiple scientific and technological project management and algorithm research work. And now, he is a senior engineer of Dispatching and Control Center of Inner Mongolia Power (Group) Co., LTD.

The authors who did not provide the photos were reluctant to publish them.